Phase-Contrast Breast-CT: Optimization of Experimental Parameters and Reconstruction Algorithms

Sandro Donato, Serena Pacile', Luca Brombal, Giuliana Tromba, and Renata Longo

Abstract

X-ray breast computed tomography (breast-CT) is a new emerging technique for breast imaging however its application is still limited because of low spatial resolution and high delivered dose. In this framework, synchrotron radiation provides ideal X-ray imaging conditions. Tunable and monochromatic laminar X-ray beam, along with large propagation distance, allows acquiring images with high quality, low scatter and dose reduction, due to the selection of the most suitable energy for the given thickness and breast composition. Moreover, the high spatial coherence permits to exploit the phase-contrast effects enabling a better image quality and soft tissue contrast. At the Elettra synchrotron facility, in Italy, a project for in vivo low-dose, high-contrast and high-resolution breast-CT is under development using a high-efficiency photon-counting detector. Due to the vertical size of the beam ($\sim$3.5 mm) the scan requires a sequence of vertical steps. Thus reducing the number of projections is essential to shorten the total acquisition time. Optimized preprocessing algorithms (phase-retrieval) and the state of the art of tomographic reconstruction methods are crucial to improve image quality. In this work, performances of standard and iterative reconstruction algorithms at different experimental conditions are compared, evaluating quantitatively the image quality in terms of Contrast-to-Noise ratio and edge sharpness. Preliminary results suggest that, in the light of a clinical exam where a short scan time is desirable, the projection number can be reduced without a major loss in image quality by applying FBP based reconstruction algorithms and phase-retrieval pre-processing.

Keywords

Breast-CT • Phase-Contrast • Reconstruction algorithms

1 Introduction

Breast cancer is one of the most common cancer in women worldwide. It also represents about a quarter of all cancers in women and the second leading cause of cancer related death [1]. The importance of early detection leads to an increasing interest in the development of novel tools and imaging techniques that may supplement or replace mammography, overcoming its limited specificity [2]. In the last few decades an increased effort in the transition from mammography to three-dimensional (3D) imaging has been made in clinical practice with the realization of 3D mammographic systems, such as tomosynthesis [3, 4] and breast-CT dedicated scanners [5, 6]. Tomosynthesis, when combined to digital mammography, leads to a significant increase in the breast cancer detection rate but at the cost of increased glandular dose [4, 7]. Cone breast CT [8] is a promising technique because it has full 3D capability with near-isotropic resolution but still limited because of low spatial resolution and high delivered dose.

In this framework, synchrotron radiation provides ideal X-ray imaging conditions. The possibility to tune monochromatic X-rays enables the selection of the most suitable energy for a given thickness and breast composition. This point represents a great benefit for both image quality and dosimetry in radiological applications [9]. The high spatial coherence enables the detection of phase effects which can be exploited for imaging biological tissues [10]. In the simplest phase sensitive imaging configuration, the so-called propagation-based imaging technique (PB-CT), to detect phase effects, it is sufficient to place the sample at a

S. Donato (✉) · L. Brombal · R. Longo
INFN Sezione Di Trieste, Trieste, Italy
e-mail: sandro.donato@elettra.eu

S. Pacile'
Department of Engineering and Architecture, University of Trieste, Trieste, Italy

S. Pacile' · G. Tromba
Elettra-Sincrotrone Trieste S.C.p.A, Basovizza, Trieste, Italy

L. Lhotska et al. (eds.), *World Congress on Medical Physics and Biomedical Engineering 2018*,
IFMBE Proceedings 68/1, https://doi.org/10.1007/978-981-10-9035-6_20

suitable distance from the detector. From the acquired projections, phase information can be exploited to improve signal-to-noise ratio of the projection by applying the phase retrieval algorithm [11].

Phase-contrast imaging has been shown to provide enhanced soft-tissue contrast and improved better visualization and characterization of lesions in breasts [12, 13]. Different feasibility studies have been recently conducted for evaluating the potentials of PB-CT to the characterization of breast tissue specimens [14–16].

In this context, the SYRMA-3D (SYnchrotron Radiaton for Mammography) aims to setup the first clinical protocol of PB-CT at the Elettra synchrotron light source in Trieste (Italy). To achieve high image quality at low delivered dose ($\sim$5 mGy mean glandular dose), both the experimental setup and the data processing include a number of innovative elements: novel high-efficiency CdTe photon-counting detector, dedicated pre-processing procedure, Phase Retrieval (PhR) algorithm and Monte Carlo model for the mean glandular dose estimation [17]. Recently, a work showing the first characterization of the imaging system and the first images of breast specimens have been published showing encouraging results in terms of image quality and delivered dose [18].

At present, a great effort is being made to reduce the total scan time which, due to the limited vertical size of the beam ($\sim$3.5 mm), the maximum frame rate of the detector (33 fps) and the selected number of projections (1200 per scan), currently is of the order of ten minutes. Considering the actual beam size and that the frame rate cannot be further increased, reducing the number of projections is the only way to shorten the total duration time of the exam. Furthermore, the role of the reconstruction algorithms in the image quality must be evaluated and discussed. In the following the image quality is established using two common metrics, namely the edge sharpness and the Contrast-to-Noise Ratio (CNR). This study is carried out using a surgical breast specimen to simulate conditions as close as possible to a clinical exam.

2 Materials and Methods

2.1 Breast Tissue Sample

The image reported in this study was acquired to guide the pathologist in the localization of lesions for the histological examination, according to the standard procedures of the Pathology Unit of the Academic Hospital of Cattinara, Trieste University, accredited by JCI (Joint Commission International). The sample was derived from surgical material sent to the Pathology Unit according to local guidelines for histological examination. The Directive 2004/23/EC of the European Parliament and of the Council of 31 March 2004 on setting standards of quality and safety for the donation, procurement, testing, processing, preservation, storage and distribution of human tissues were followed. For breast-CT acquisition, the sample was formalin fixed and sealed hermetically in a polyethylene container. The dimensions of the specimen, containing an infiltrating ductal carcinoma, were approximately 10 cm by 8.5 cm and the thickness was of about 4 cm.

2.2 Experimental Setup and Acquisition Parameters

Breast-CT scans were performed the SYRMEP (SYnchrotron Radiation for MEdical Physics) beamline of Elettra. X-rays are generated by a bending magnet in the energy range from 8.5 to 40 keV, while energy is selected using a Si (111) double-crystal monochromator with resolution of $\Delta E/E \approx 10^{-3}$. The beam cross-section at sample position is 220 (horizontal) $\times$ 3.5 mm (vertical, Gaussian shape, FWHM). CT projections are acquired using a photon-counting detector (PIXIRAD-8), made up by 8 adjacent modules with a CdTe sensor, a pixel spacing of 60 μm and a global active area of 246 $\times$ 25 mm^2 (4096 $\times$ 476 pixels). It is placed in the beamline patient room 32 m far away from the X-ray source. Sample is attached to a rotating bed in correspondence of an ergonomic aperture devoted to host the breast of the patient. The sample-to-detector distance is 1.6 m that allows to detect phase-contrast effects.

Due to the small beam divergence ($\sim$7 mrad), scans were done over 180 degrees, at the maximum frame rate of the detector in dead-time-free mode [19], collecting 1200 equally-spaced projections at three different energies (32, 35 and 38 keV) of the same region of the tissue. The photon beam was filtered with Aluminum sheets of different thickness to deliver a fixed Mean Glandular Dose (MGD) of 5 mGy, that is a dose comparable with a two views mammographic exam. The MGD's was calculated according an ad hoc developed model [17] based on a MonteCarlo simulation developed and validated for this program [20].

2.3 Data Pre-processing and Reconstruction

Starting from the original stacks of projections, two new datasets with 600 and 900 images were generated by means of linear interpolation, preserving the delivered MGD. Raw collected images undergo to an optimized pre-processing procedure that performs dynamic flat fielding equalization [21], fix gaps around adjacent modules, applies despeckle and dynamic ring removal filters. Subsequently a

single-distance phase-retrieval algorithm, based on the Homogeneous Transport of intensity equation (TIE-Hom [11]), is applied. The algorithm requires as input parameter the δ/β ratio, whereas δ and β denote, the phase-shift and the absorption components of the complex refractive index $n = 1 - \delta + i\beta$, respectively. We used two distinct δ/β ratios, the first value is theoretical value [22] of breast tissue in air ($\delta/\beta \sim 2300$, hereafter single material PhR), while the latter considers an adipose/glandular tissues interface (δ/β = 870, 978, 1083 for 32, 35 and 38 keV, respectively, hereafter two material PhR). Then the slices have been reconstructed with an in-house built software [23] using different GPU-based reconstruction algorithms: standard Filtered Back Projection (FBP), Simultaneous Iterative Reconstruction Technique (SIRT) using 1000 iterations, Simultaneous Algebraic Reconstruction Technique (SART) with 50 iterations, and Minimum Residual Filtered Back Projection method (MR-FBP).

2.4 Quantitative Analysis

Quantitative analysis was conducted to study the influence of each parameter (energy, δ/β ratio, number of projections and reconstruction algorithm) on the quality of the reconstructed images. We evaluated image quality using two estimators: Contrast-to-Noise Ratio (CNR) and edge sharpness. CNR helps to evaluate the visibility of low-contrast structures and is defined as:

$$CNR = \frac{|S_g - S_a|}{\sqrt{(\sigma_g^2 + \sigma_a^2)/2}} \quad (1)$$

where S is the mean value of a homogeneous region of interest (ROI), σ is the associated standard deviation and the subscripts g and a refer to glandular and adipose tissues. The CNR was measured taking the average CNR of four non-overlapping pairs of square ROIs (showed with square boxes in Fig. 1), where for each pair one ROI is selected within the glandular tissue and the other within the adipose tissue.

Edge sharpness was evaluated by fitting an error function (erf) in a profile (shown with the magenta line in Fig. 1) of the interface between adipose and glandular tissue, across a sharp step-wedge (produced by a surgical cut during the preparation for formalin fixation), calculating the derivative of this function (a Gaussian) and measuring the full width at half maximum value (FWHM). The error associated to the measured resolution is derived from the parameter uncertainty with the error propagation rules.

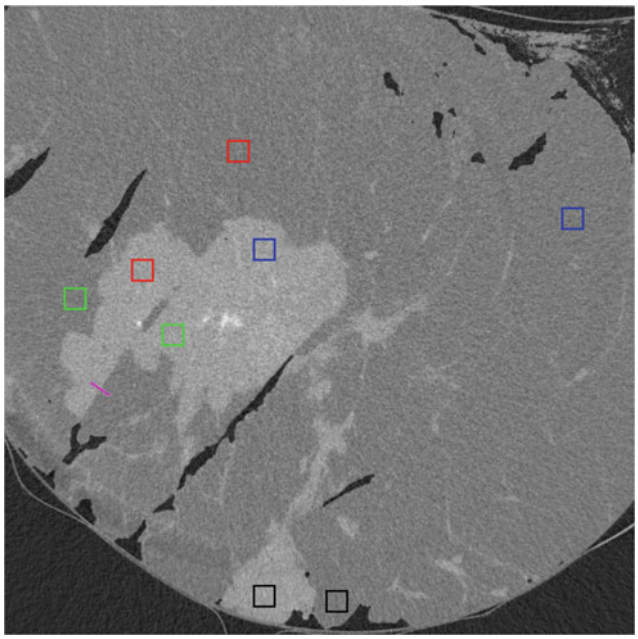

Fig. 1 Slice of the central region of the breast tissue at 32 keV reconstructed with FBP, using 1200 projections and δ/β = 2308. Squares represent ROIs for the evaluation of the CNR. Different colors indicate a different couple of glandular-adipose uniform regions. The magenta line refers to the edge used for spatial resolution evaluation

3 Results and Discussion

Results of the quantitative analysis, for the single and two material PhR, are reported in Tables 1 and 2, respectively. In Table 1 the CNR and FWHM for all the energies, projection numbers and reconstruction algorithms, when the single material PhR is applied, are reported. Comparing the algorithms while keeping the number of projection fixed, it can be noted that SIRT reconstructions have the best CNR but the poorest resolution, while FBP gives the best spatial resolution with the lowest CNR (Fig. 2a–d). Furthermore, regardless of the reconstruction algorithm, reducing the number of projections the spatial resolution worsens; on the contrary the CNR remains constant if FBP is applied while it increases for the other algorithms (see Fig. 3). Comparing the energies, it is shown that the 38 keV reconstruction gives the lowest CNR while the values at 32 and 35 keV are comparable.

When the two materials PhR is applied (Table 2), CNR and FWHM show similar dependence on the reconstruction algorithms and projection numbers as observed in Table 1. Contrarily, the CNR shows a little energy dependence and its values are compatible within the statistical uncertainty for all the energies.

Table 1 Values of CNR and FWHM for single material PhR, at different energies, number of projections and reconstruction algorithm

N_{proj}	Algorithm	E = 32 keV		E = 35 keV		E = 38 keV	
		CNR	FWHM (mm)	CNR	FWHM (mm)	CNR	FWHM (mm)
1200	FBP	3.62 ± 0.15	0.13 ± 0.03	3.55 ± 0.26	0.11 ± 0.06	3.11 ± 0.22	0.13 ± 0.03
	MR-FBP	4.31 ± 0.14	0.15 ± 0.02	4.18 ± 0.26	0.12 ± 0.05	3.72 ± 0.21	0.13 ± 0.02
	SART	3.29 ± 0.13	0.17 ± 0.02	3.65 ± 0.36	0.12 ± 0.05	3.17 ± 0.16	0.13 ± 0.02
	SIRT	7.02 ± 0.18	0.25 ± 0.01	7.03 ± 0.38	0.21 ± 0.03	6.30 ± 0.29	0.25 ± 0.01
900	FBP	3.65 ± 0.15	0.15 ± 0.03	3.62 ± 0.33	0.13 ± 0.06	3.18 ± 0.29	0.16 ± 0.03
	MR-FBP	4.92 ± 0.11	0.19 ± 0.02	4.87 ± 0.32	0.14 ± 0.04	4.32 ± 0.27	0.18 ± 0.02
	SART	4.38 ± 0.22	0.17 ± 0.02	4.24 ± 0.31	0.20 ± 0.03	3.52 ± 0.27	0.18 ± 0.02
	SIRT	7.21 ± 0.23	0.27 ± 0.01	7.32 ± 0.42	0.22 ± 0.03	6.49 ± 0.36	0.28 ± 0.02
600	FBP	3.56 ± 0.05	0.16 ± 0.02	3.52 ± 0.25	0.17 ± 0.07	3.15 ± 0.27	0.18 ± 0.05
	MR-FBP	6.11 ± 0.28	0.22 ± 0.01	6.22 ± 0.28	0.18 ± 0.03	5.60 ± 0.39	0.21 ± 0.02
	SART	5.64 ± 0.33	0.22 ± 0.01	5.89 ± 0.42	0.22 ± 0.03	5.19 ± 0.23	0.22 ± 0.01
	SIRT	7.59 ± 0.53	0.28 ± 0.01	8.09 ± 0.29	0.27 ± 0.02	7.28 ± 0.43	0.31 ± 0.01

Table 2 Values of CNR and FWHM for two materials PhR, at different energies, number of projections and reconstruction algorithm

N_{proj}	Algorithm	E = 32 keV		E = 35 keV		E = 38 keV	
		CNR	FWHM (mm)	CNR	FWHM (mm)	CNR	FWHM (mm)
1200	FBP	1.88 ± 0.11	0.09 ± 0.02	2.02 ± 0.17	0.09 ± 0.11	1.88 ± 0.15	0.09 ± 0.04
	MR-FBP	2.44 ± 0.11	0.13 ± 0.02	2.51 ± 0.18	0.10 ± 0.07	2.38 ± 0.15	0.11 ± 0.03
	SART	1.86 ± 0.11	0.17 ± 0.03	20.1 ± 0.16	0.11 ± 0.07	2.04 ± 0.20	0.11 ± 0.03
	SIRT	4.37 ± 0.13	0.20 ± 0.02	4.51 ± 0.31	0.17 ± 0.04	4.25 ± 0.24	0.18 ± 0.02
900	FBP	1.91 ± 0.12	0.09 ± 0.03	2.07 ± 0.21	0.12 ± 0.11	1.95 ± 0.20	0.14 ± 0.05
	MR-FBP	2.93 ± 0.11	0.18 ± 0.03	3.04 ± 0.25	0.12 ± 0.06	2.85 ± 0.21	0.14 ± 0.03
	SART	2.66 ± 0.08	0.17 ± 0.04	2.69 ± 0.22	0.12 ± 0.06	2.37 ± 0.22	0.14 ± 0.02
	SIRT	4.59 ± 0.11	0.21 ± 0.02	5.38 ± 0.35	0.18 ± 0.04	4.49 ± 0.32	0.21 ± 0.02
600	FBP	1.86 ± 0.03	0.14 ± 0.03	2.01 ± 0.17	0.13 ± 0.10	1.92 ± 0.17	0.15 ± 0.06
	MR-FBP	3.87 ± 0.06	0.22 ± 0.02	4.01 ± 0.23	0.15 ± 0.05	3.83 ± 0.29	0.18 ± 0.02
	SART	3.57 ± 0.17	0.22 ± 0.02	3.91 ± 0.28	0.17 ± 0.05	3.45 ± 0.20	0.17 ± 0.02
	SIRT	5.03 ± 0.15	0.23 ± 0.01	5.39 ± 0.25	0.21 ± 0.04	5.12 ± 0.35	0.24 ± 0.02

In general, comparing results at different δ/β, the single material approach produces a higher CNR (40% in average) and a worst spatial resolution (20% in average). These effects can be seen in Fig. 4 that compares FBP reconstructions with different δ/β ratio. The one with a lower δ/β ratio has sharpen edges, but it looks noisy. On the contrary, the appearance of the slice at higher δ/β is better (higher visibility of glandular blanches). In order to better visualize results reported in the tables, scatter plots of the FWHM vs CNR at 32 keV for both δ/β ratios are presented in Fig. 5. In a recent work [24] it was established that if an insufficient CNR is detected, a radiologist judges an image as meaningless for the diagnosis process. Beyond a level of CNR considered acceptable, the radiologists prefer the images having the highest edges sharpness (i.e. the lowest value of FWHM). Therefore, as an example, SIRT algorithm produces a major CNR increment while introducing a substantial blurring (see Fig. 2d) has not to be considered for our study. The SART algorithm, while enhancing CNR with good spatial resolution, introduces a texturized noise in the reconstruction (see Fig. 2c). The MR-FBP, at least for 900 and 1200 projections, shows a spatial resolution comparable to FBP, giving at the same time a better CNR (see Fig. 2a–b).

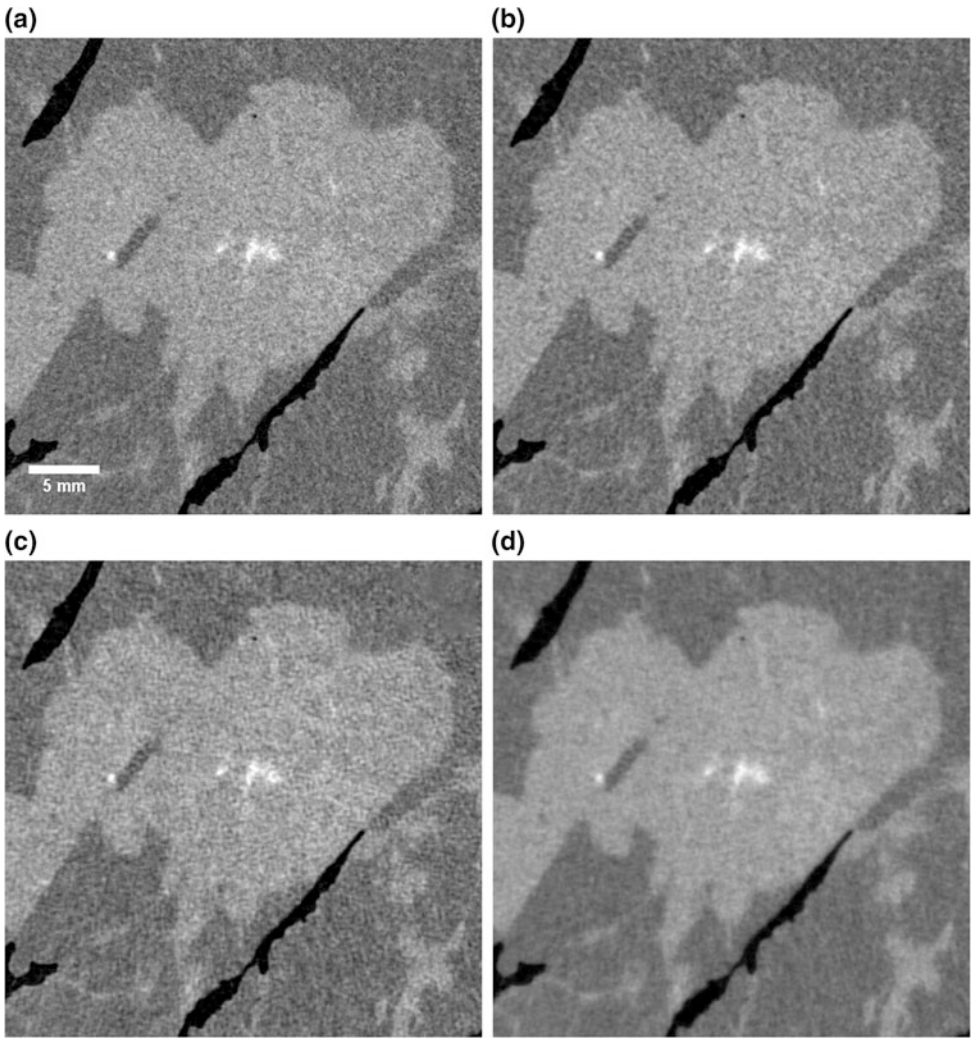

Fig. 2 Detail of the central region of a slice reconstructed with FBP (**a**), MR-FBP (**b**), SART (**c**) and SIRT (**d**) algorithms, acquired at 32 keV using 1200 projections and $\delta/\beta = 2308$ (slices are showed with the same grayscale range). The white pixels indicate a calcification inside the lesion (bright gray) surrounded by adipose tissue (dark gray). Sharp edges and air (black regions) are a result of the surgical cuts done for clinical assessment. FBP slice **a** appears sharper than the ones resulting from other reconstructions, but at the same time with higher noise, while SIRT slice **d** is clearer visible, i.e. with more CNR, but more blurred

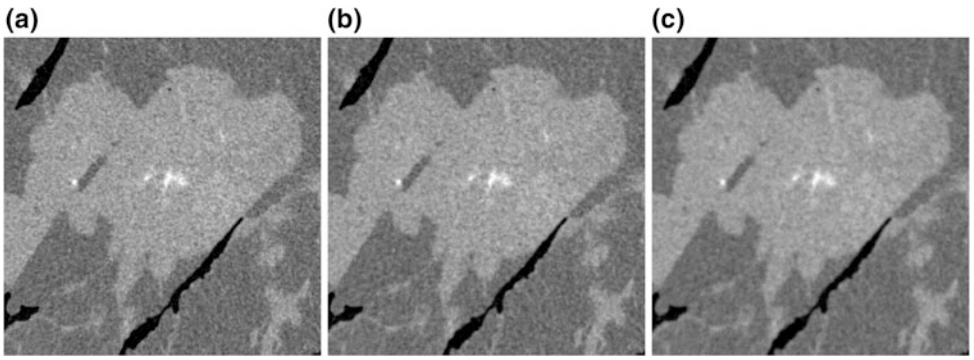

Fig. 3 Different panels shown MR-FBP slices with different number of projections, 1200 (**a**), 900 (**b**) and 600 (**c**), respectively. With non-standard reconstruction algorithms, reducing the number of projections increases the CNR and decreases the spatial resolution

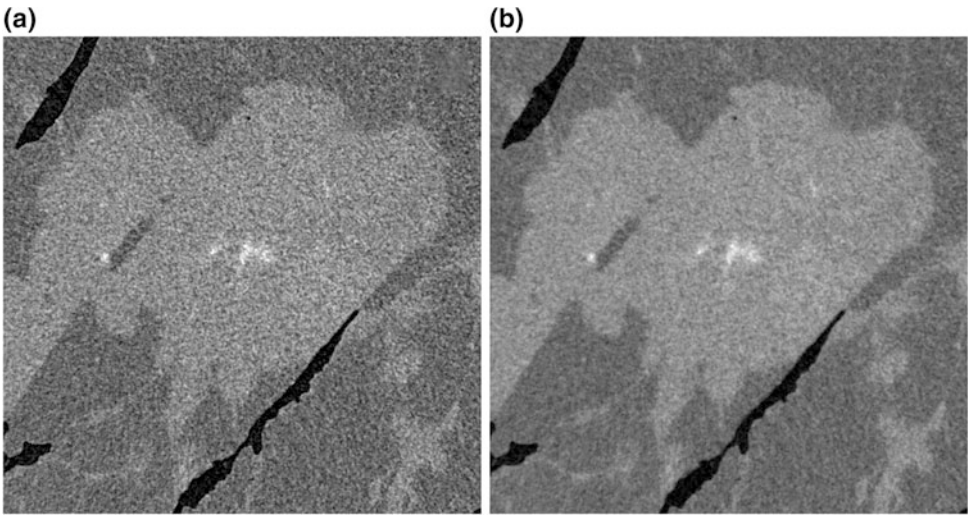

Fig. 4 FBP reconstructions, at 32 keV and 1200 projections, with two materials **a** and single material **b** PhR

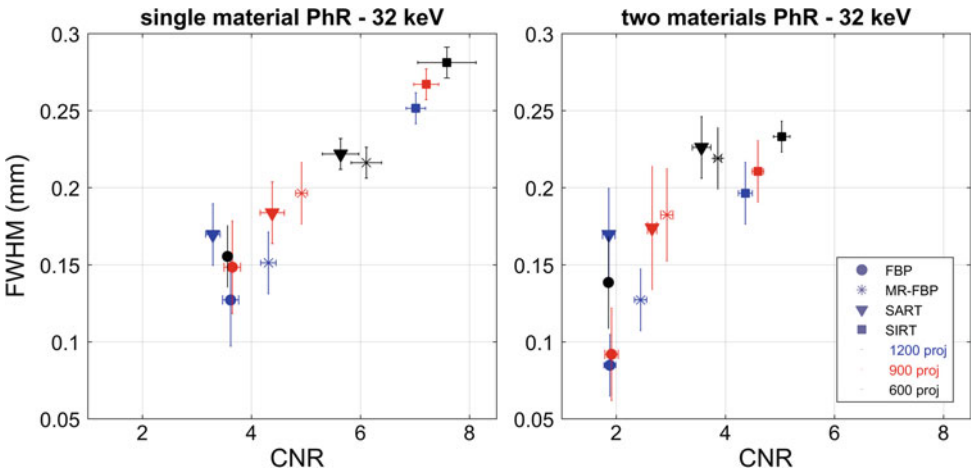

Fig. 5 Scatter plot of the FWHM and CNR at 32 keV with single material PhR (left) and two materials PhR (right). Different symbols denote different algorithms, while colors indicate the number of projections used for reconstruction (1200 in blue, 900 in red, 600 in black)

4 Conclusions

In this study we report PB-CT images of a large ($\sim$ 10 cm in diameter) breast specimen acquired with a delivered dose (5 mGy MGD) lower than (or comparable to) available clinical systems but with higher spatial resolution (60 um pixel size and FWHM down to 100 um). Two different sets of δ/β ratio are compared, showing that, for a given CNR, the single material approach results in a better spatial resolution (see Fig. 3).

The performances of different reconstruction algorithms were investigated: in general, an increase in CNR is related to a decrease of the spatial resolution. The best spatial resolution is obtained using the FBP while similar performances, with a slight increase in CNR, are produced by the MR-FBP. On the contrary, the iterative algorithms produce a major increase in CNR but they introduce either a textured noise (SART) or an excessive blurring (SIRT).

In the selected energy range (32–38 keV) the CNR is slightly energy dependent, reporting the highest values for energies lower or equal 35 keV.

In the light of a clinical breast-CT exam, where a short scan time is desirable, the projection number can be reduced down to 900 without a major loss in image quality by applying the FBP-based reconstruction algorithms and single material PhR.

In this work preliminary results are presented and a wider study comprising several breast samples, a larger energy range and an image scoring by radiologists is ongoing to perform the final tuning of phase retrieval and reconstruction parameters.

Acknowledgements Funding: This work was conducted within the SYRMA-3D project, which is funded by Istituto Nazionale di Fisica Nucleare (National Scientific Committee 5 for Technological and Inter-Disciplinary research) and supported by Elettra-Sincrotrone Trieste S.C.p.A. S. Donato was partially supported by Consorzio per la Fisica Trieste. The authors acknowledge Prof. F. Zanconati MD and Dr

Deborah Bonazza MD for providing and preparing the breast specimen. Authors want also to thank all the participant of the SYRMA-3D collaboration for their support and useful discussions. We thank the staff of the SYRMEP beamline for the precious help during the experimental activity.

Compliance with Ethical Requirements The authors declare that they have no conflict of interest.

References

1. Siegel, R.L., Miller, K. D., Jemal, A.: Cancer statistics, 2016. CA: a cancer journal for clinicians 66, 7–30 (2016).
2. Sprague, B. L., Arao, R. F., Miglioretti, D. L., et al.: National performance benchmarks for modern diagnostic digital mammography: Update from the breast cancer surveillance consortium, 283, 59–69 (2017).
3. Teertstra, H.J., Loo, C.E., van den Bosch, M.A.A.J., et al.: Breast tomosynthesis in clinical practice: initial results. European Radiology 20, 16–24 (2010).
4. Sechopoulos, I.: A review of breast tomosynthesis. Part I. The image acquisition process. Med. Phys. 40, 014301–12 (2013).
5. O'Connell, A.M., Karellas, A., Vedantham, S.: The potential role of dedicated 3D breast CT as a diagnostic tool: review and early clinical examples. Breast J. 20, 592–605 (2014).
6. Zhao, B., Zhang, X., Cai, W., Conover, D., Ning, R.: Cone beam breast CT with multiplanar and three dimensional visualization in differentiating breast masses compared with mammography. Eur. J. Radiol. 84, 48–53 (2015).
7. Olgar, T. Kahn, T., Gosch, D.: Average glandular dose in digital mammography and breast tomosynthesis. Rofo, 184 (10), 911–918 (2012).
8. Lindfors, K.K., Boone, J.M., Nelson, T.R., Yang, K., Kwan, A.L., Miller, D.F.: Dedicated breast CT: initial clinical experience. 246 (3), 725–33 (2008).
9. Fedon, C.,Rigon, L., Arfelli, F., et al.: Dose and diagnostic performance comparison between phase-contrast mammography with synchrotron radiation and digital mammography: a clinical study report. JMI (2018) in press.
10. Beltran, M.A., Paganin, D.M., Siu, K. K.W., et al.: Interface-specific x-ray phase retrieval tomography of complex biological organs, Phys.Med.Biol. 56(23), 7353–69 (2011).
11. Paganin, D., Mayo, S., Gureyev, T. E., Miller, P. R., and Wilkins, S. W.: Simultaneous phase and amplitude extraction from a single defocused image of a homogeneous object. J. Microsc. 206(1), 33–40 (2002).
12. Longo, R., Tonutti, M., Rigon, L., et al.: Clinical study in phase-contrast mammography: image-quality analysis. Philos. Trans. A. Math. Phys. Eng. Sci. 372, 20130025 (2010).
13. Coan, P., Bravin, A., Tromba, G.: Phase-contrast x-ray imaging of the breast: recent developments towards clinics. J. Phys. D: Appl. Phys 46(49) 494007 (2013).
14. Zhao, Y., Brun, E., Coan, P., Huang, Z, et al.: *High-resolution, low-dose phase contrast X-ray tomography for 3D* diagnosis of human breast cancers. Proc. Nat. Acad. Sci. 109(45), 18290–18294 (2012).
15. Nesterets, Y.I., Gureyev, T.E., Mayo, S.C., et al.: A feasibility study of x-ray phase-contrast mammographic tomography at the imaging and medical beamline of the australian synchrotron. J. Synch. Rad. 22, 1509–1523 (2015).
16. Baran, P., Pacilè, S., Nesterets, Y., et al.: Optimization of propagation-based x-ray phase-contrast tomography for breast cancer imaging. Phys. Med. Biol. 62, 2315–2332 (2017).
17. Mettivier, G., Fedon, C., Di Lillo, F., et al.: Glandular dose in breast computed tomography with synchrotron radiation. Phys. Med. Biol. 61(2), 569 (2016).
18. Longo, R., Arfelli, F., Bellazzini, et. al: Towards breast tomography with synchrotron radiation at Elettra: first images. Phys. Med. Biol. 61(4), 1634 (2016).
19. Delogu, P., Golosio, B., Fedon, C., et al.: Imaging study of a phase-sensitive breast-CT system in continuous acquisition mode. J. Instr. 12(01), C01016 (2017).
20. Fedon, C., Longo, F., Mettivier, G., Longo, R.: Geant4 for breast dosimetry: parameters optimization study. Phys. Med. Biol. 60 (16), N311 (2015).
21. Delogu, P., Brombal, L., Di Trapani, V., Donato, et al.: Optimization of the equalization procedure for a single-photon counting CdTe detector used for ct. J. Instr. 12(11), C11014 (2017).
22. TS_imaging Homepage: https://ts-imaging.net/Services/Simple/ICUtilXdata.aspx.
23. Brun, F., Pacilè, S., Accardo, A., et al.: Enhanced and flexible software tools for x-ray computed tomography at the italian synchrotron radiation facility Elettra. Fundam. Inform. 141(2–3), 233-243 (2015).
24. Pacilè, S., Brun, F., Dullin, C., et al.: Clinical application of low-dose phase contrast breast CT: methods for the optimization of the reconstruction workflow. Biomed. Opt. Expr. 6(8), 3099–3112 (2015).